Structure and Properties of Organoclay/EPDM Nanocomposites: Influence of Ethylene Contents

Yong Ma, You-Ping Wu, Yi-Qing Wang, Li-Qun Zhang

Key Laboratory for Nanomaterials, Ministry of Education, The Key Laboratory of Beijing City for Preparation and Processing of Novel Polymer Materials, Beijing University of Chemical Technology, Beijing 100029, China

Received 21 March 2005; accepted 15 May 2005
DOI 10.1002/app.22247
Published online in Wiley InterScience (www.interscience.wiley.com).

ABSTRACT: Four organoclay (OC)/ethylene–propylene–diene rubber (EPDM) nanocomposites with different ethylene contents were prepared by melt blending. X-ray diffraction spectrum (XRD) and transmission electronic microscope (TEM) photos showed that OC/EPDM nanocomposites were intercalated, and the ethylene content had little influence on the dispersion of OC. The addition of OC prolonged the optimum cure time and reduced the crosslink density of OC/EPDM. The improvement in tensile strength of OC/EPDM nanocomposites with high ethylene contents (67–70%) was larger than that of OC/EPDM nanocomposites with low ethylene contents (52–52.5%). XRD results of the stretched samples testified that the extension promoted orientation of silicate layers, and induced crystallization of polyethylene (PE) segments in OC/EPDM nanocomposites with high ethylene contents. The highly oriented microfibrillar structure and more oriented amorphous chains, which resulted from strain-induced crystallization of PE segments and the orientation of clay layers in OC/EPDM nanocomposites with high ethylene contents (67–70%), should be responsible for larger improvement in tensile strength than that of those nanocomposites with low ethylene contents (52–52.5%) © 2005 Wiley Periodicals, Inc. J Appl Polym Sci 99: 914–919, 2006

Key words: ethylene content; EPDM; nanocomposite; organoclay; strain-induced crystallization

INTRODUCTION

Since the successful preparation of montmorillonite/PA nanocomposite by Usuki et al.[1] for the first time, a large number of montmorillonite/polymer nanocomposites have been prepared. Compared with the conventional microcomposite counterparts, these nanocomposites have outstanding mechanical properties,[2,3] thermal stability,[4] gas barrier property,[5] etc. The preparation methods mainly include in situ polymerization,[6,7] solution blending,[8,9] melt blending,[10] and latex method.[11] Among these four methods, the latex route is promising for polymers having a latex form because pristine clay can be directly used, whereas melt compounding, a conventional processing method, is more convenient and versatile.

Since ethylene–propylene–diene rubber (EPDM) does not have a latex form, layered silicate/EPDM nanocomposites are mainly prepared by melt blending method. EPDM, as a kind of rubber with high saturation, does not have any polar groups in its backbone, and thus, it is difficult for EPDM molecules to intercalate into and exfoliate montmorillonite layers in them. However, Chang et al.,[12] Usuki et al.,[13] and Zheng et al.[14] have successfully prepared organomontmorillonite/EPDM nanocomposites by melt method, which exhibit high tensile strength. The effects of the types of surfactants and vulcanization accelerators on the morphology and properties of these nanocomposites have been investigated.

In this paper, influence of the ethylene content in EPDM on the morphology and properties of organoclay (OC)/EPDM nanocomposites prepared by melt method were investigated. The results are expected to provide an insight into the cause of high tensile strength of these nanocomposites.

EXPERIMENTAL

Materials

EP33 was purchased from Japan Synthetic Rubber Co. Ltd. (JSR). J4045, J2080, and J3080 were supplied by Jilin Chemical Industrial Co. Ltd. (China), and the related characteristic data are shown in Table I. OC (montmorillonite modified by octadecyltrimethyl ammonium, interlayer distance: 2.3 nm) was from Lin'an

Correspondence to: L.-Q. Zhang (zhangliqunghp@yahoo.com).

Contract grant sponsor: National Tenth-five Program; contract grant number: 2001BA310A12.
Contract grant sponsor: Key Project of Beijing Natural Science Foundation; contract grant number: 2031001.
Contract grant sponsor: Beijing New Star Plan Project; contract grant number: 2004A14.

TABLE I
Characteristic Data of EPDMs[a]

Sample	The third monomer[a]	Iodine value[a]	Ethylene content (%)[a]	Mooney viscosity ML_{1+4}, at 100°C[b] (Mooney point)	Molecular weight distributions
J4045	ENB	25	52.5	48	Broad
EP33	ENB	26	52	51	Broad
J2080	ENB	12	67	86	Narrow
J3080	ENB	11	70	92	Narrow

[a] Supplied by the manufacturers.
[b] Measured by rheometer Rheograph M3810C from Beijing Huanfeng Chemical Industry Machine Experiment Factory (China).

paint additives factory (China). Other compounding ingredients were commercial-grade products.

Preparation of OC/EPDM nanocomposite

EPDM (100 phr) and OC (10 phr) were mixed on an open two-roll mill for about 10 min at 100°C, and the mixture was obtained. After that, 1.2 phr zinc diethyl dithiocarbamate (ZDC), 5 phr zinc oxide (ZnO), 1 phr stearic acid (SA), and 1.5 phr sulfur were added to the mixture on a two-roll mill at room temperature; the compounds were vulcanized in a standard mold for t_{90} at 160°C under certain pressure. Disk rheometer P355B2 produced by Beijing Huanfeng Chemical Industry Machine Experiment Factory (China) was used to measure optimum cure time (t_{90}).

Characterization

X-ray diffraction (XRD) was carried out using a diffractometer (D/Max-III C, Rigaku, Japan) with CuK-α radiation, operating at 40 kV and 200 mA. Basal spacing between silicate layers of OC and OC/EPDM nanocomposites was observed from 0.5° to 10° (2θ) at a scan rate of 1°/min, while OC orientation and polyethylene (PE) segment crystal in OC/EPDM during the tensile process were observed on the stretched samples at different elongations from 3° to 90° (2θ) at a scan rate of 10°/min.

Transmission electron microscopy (TEM) observations were performed on the ultrathin sections with a H-800 TEM (Hitachi, Japan) at an acceleration voltage of 200 kV at room temperature, and the ultrathin sections were prepared with a cryo-ultramicrotome under liquid nitrogen cooling.

Measurement of mechanical properties

Tensile tests were carried out on CMT4104 electric tensile tester (SANS, Shenzhen, China) according to ASTM standards, and the strain–stress curves were drawn simultaneously.

RESULTS AND DISCUSSION

Structure of OC/EPDM nanocomposites

Figure 1 shows the XRD curves of OC and four kinds of OC/EPDM nanocomposites using EP33, J4045, J2080, and J3080 as the matrix, respectively. The peaks shown in these XRD curves correspond to the (001) plane reflections of OC. The basal spacing of OC is about 2.0 nm, whereas the interlayer distances of the four OC/EPDM nanocomposites are about 4.6–4.7 nm, indicating that some rubber macromolecules are intercalated into the intergallery. Since EPDM macromolecules have no polar groups, it seems to be very difficult for EPDM to intercalate into the interlayer to enhance the spacing to as much as 4.6–4.7 nm. However, besides the characteristics of rubber,[15] the intercalation process is also closely related to the type of modifiers,[16] the type of vulcanization accelerators,[13] the processing conditions,[17] *etc*. According to the literature,[16] using quaternary ammonium as the modifier, layer distance of the intercalated structure of EPDM/OC nanocomposites in the case of accelerator ZDC was larger than that with primary ammonium intercalant, although addition of OC modified by primary ammonium was easier to induce better clay

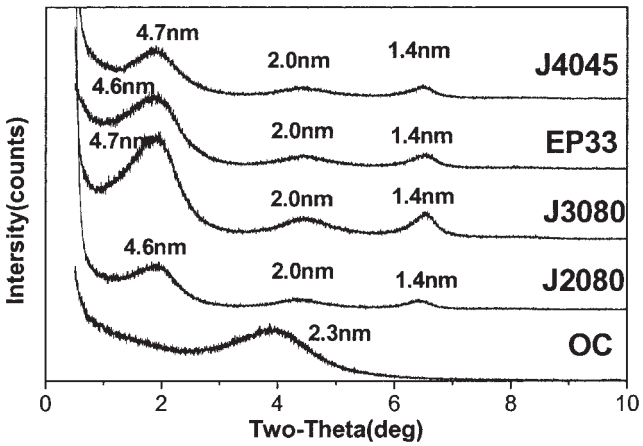

Figure 1 XRD patterns of OC and EP33, J4045, J2080, and J3080/OC nanocomposites.

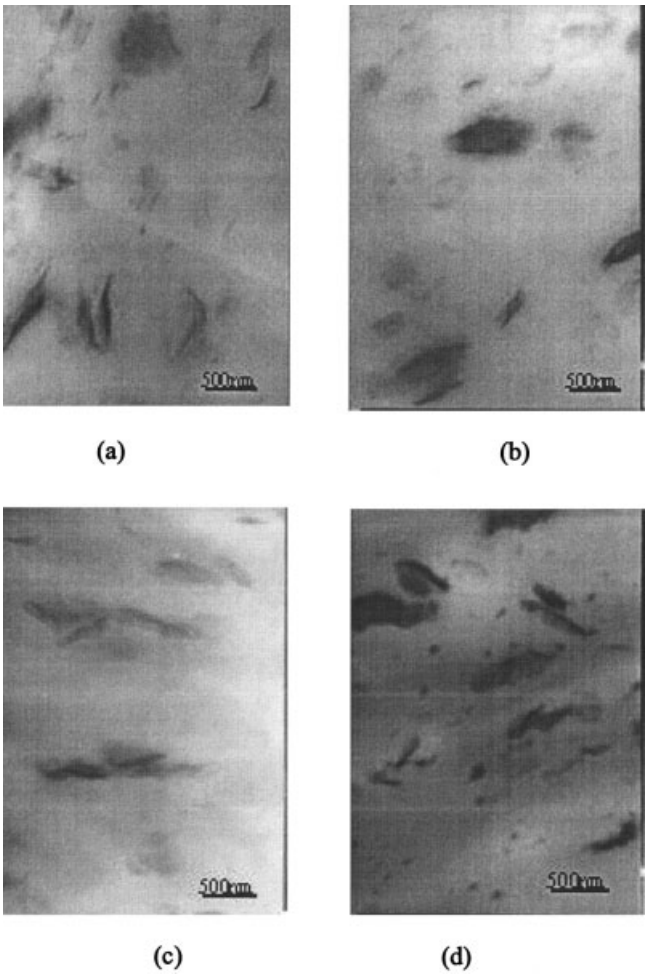

Figure 2 TEM photographs of nanocomposites (10/100): (a) OC/EP33, (b) OC/J4045, (c) OC/J2080, and (d) OC/J3080.

dispersion *via* layers separation or declamination/exfoliation, because of the possible reaction between primary ammonium and zinc dialkyl dithiocarbamate. In addition, our experiments were performed on roll mill, different from the internal mixer, which should contribute to the higher interlayer spacing.

In Figure 1, the peaks at 2.0 and 1.4 nm, lower than the initial value of OC (2.3 nm), are also noticed. The same phenomenon has widely been observed in rubber/OC nanocomposites, by other researchers.[10,16] This may be due to deintercalation of the clay galleries.

TEM photos of the four OC/EPDM nanocomposites are shown in Figure 2, in which the black lines are the section of clay layers. From Figure 2, it can be seen that the majority of intercalated clay layers (XRD results) in the four nanocomposites are not exfoliated. Though ethylene content in four EPDM matrices is different, the dispersion level of OC is almost the same. This is assignable to the fact that ethylene and propylene are both nonpolar monomers. According to the results of XRD and TEM, there is little difference in the dispersion level of OC in the four EPDM matrices

Curing behavior of OC/EPDM nanocomposites

The effects of OC on the curing behavior of OC/EPDM nanocomposites are shown in Table II. The lowest torque (ML) value of OC/EPDM nanocomposites in vulcanization curves is higher than that of the corresponding pure EPDM, indicating that the incorporation of OC increases the viscosity of compounds. However, the maximum torque (MH) is lower than that of the corresponding pure EPDM, and moreover, the optimum cure time of OC/EPDM is significantly prolonged relative to that of the corresponding pure EPDM. These results suggest that the crosslink density of OC/EPDM is reduced by addition of OC, presumably owing to the adsorption of curing agents on the filler surface. This result agrees well with the findings of other researchers, on the OC/EPDM composites.[14]

Mechanical properties

The mechanical properties of OC/EPDM nanocomposites with different ethylene contents are shown in Table III. Because of the addition of OC, the mechanical properties of the four OC/EPDM nanocomposites, including hardness, tensile strength, elongation-at-break, and tear strength, are all improved relative to those of the corresponding pure EPDM. Two points are worthy to be noted: (a) Compared to pure EPDM vulcanizates, the elongation-at-break of OC/EPDM nanocomposites is evidently improved and the permanent set is larger. These phenomena should be attributed to the decrease in crosslink density resulting in the increase of macromolecule chain slippage during the tensile process. Owing to the same reason, EP33 and J4045 have lower elongation-at-break and permanent set than J2080 and J3080. Since the iodine values of EP33 and J4045 are higher than those of J2080 and J3080, the crosslink density of EP33 and J4045 should also be higher than that of J2080 and J3080, with the same amount of curing agents. OC/EPDM

TABLE II
Influence of OC on the Curing Behavior of OC/EPDM Nanocomposites

Sample	ML (dNm)	MH (dNm)	t_{90} (min)
EP33	5.12	38.68	17.5
OC/EP33	5.99	33.63	36.4
J4045	5.16	35.38	19.7
OC/J4045	6.06	30.82	37.7
J2080	11.29	42.47	20.9
OC/J2080	12.01	35.44	39.7
J3080	12.18	48.40	18.6
OC/J3080	13.92	44.11	36.2

TABLE III
Mechanical Properties of EPDM and OC/EPDM Composites

Sample	Shore A hardness	Stress at 100%/300% (MPa)	Tensile strength (MPa)	Elongation-at-break (%)	Permanent set (%)	Tear strength (kN/m)
EP33	48	1.1/-	1.4	170	0	11.0
OC/EP33	49	1.0/1.8	2.5	418	12	18.4
J4045	49	1.0/-	1.7	240	0	11.6
OC/J4045	49	1.0/1.6	2.7	505	20	17.2
J2080	52	1.0/1.7	1.9	338	4	13.1
OC/J2080	54	1.0/1.4	12.8	956	60	22.3
J3080	61	1.4/2.8	4.1	392	28	17.3
OC/J3080	66	1.8/2.9	14.9	562	64	31.4

nanocomposites exhibit the same trend, that is, OC/J2080 and OC/J3080 perform higher elongation-at-break and permanent set than OC/EP33 and OC/J4045. (b) The improvement in tensile strength of OC/J2080 and OC/J3080 nanocomposites with high ethylene contents (67–70%) is much larger than that of OC/EP33 and OC/J4045 nanocomposites with low ethylene contents (52–52.5%). To clarify the origin of this result, the stress–strain curves are plotted as shown in Figures 3 and 4.

The initial part of stress–strain behavior of OC/EPDM nanocomposites is almost the same as that of the corresponding pure EPDM. However, at large strains, the stress of OC/J2080 and OC/J3080 increases sharply in small range of strains, whereas OC/EP33 and OC/J4045 do not exhibit the same behavior. According to the literature,[18] the lightly crosslinked, ethylene-rich, random EPDM terpolymers can crystallize upon stretching, and thus, the large increase in the tensile stress of OC/J2080 and OC/J3080 may be related to the strain-induced crystallization of ethylene segments in EPDM containing high ethylene contents at the presence of intercalated OC.

Influence of tension on the microstructure

To further clarify the reinforcement mechanism of the strain-induced crystallization of ethylene segments in OC/EPDM nanocomposites, the structures of OC/J2080 (ethylene content = 67%) and OC/EP33 (ethylene content = 52%) nanocomposites during the tensile process were characterized by XRD.

XRD curves of OC/J2080 nanocomposite at different elongations are shown in Figure 5. From Figure 5, it can be seen that, compared to the XRD curve before stretching, the intensity of the characteristic peaks of clay layers at 4.8 nm representing the intercalated structure (2.0 and 1.4 nm corresponding to the deintercalation of clay galleries as described earlier) enhances with the increase in strain, indicating that the clay layers arrange more orderly during extension, whether they were intercalated or not. This result is consistent with a high degree of orientation of silicate layers under uniaxial tension in butadiene rubber or styrene–butadiene rubber containing organic layered silicates, which was monitored by means of online WAXS measurements.[19]

At the same time, the peak at about 19° in Figure 5(a) corresponds to amorphous PE.[18] Upon stretching

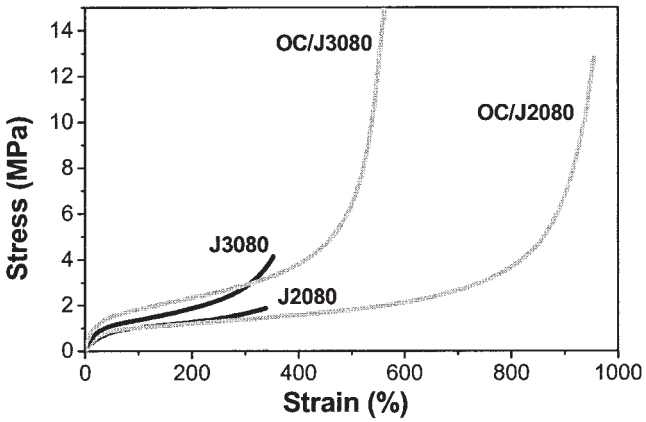

Figure 3 Strain–stress curves of OC/EPDM nanocomposites with high ethylene contents.

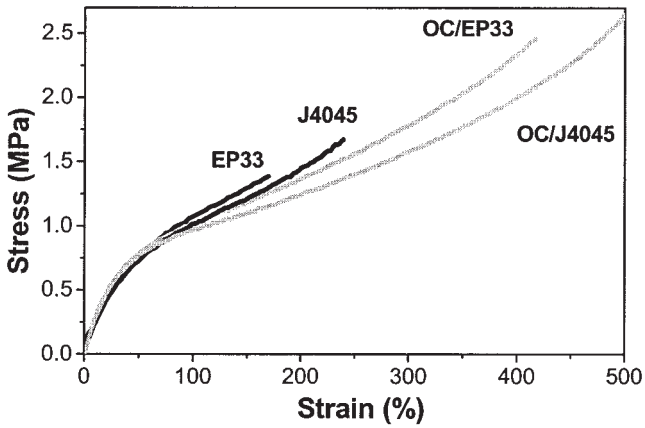

Figure 4 Strain–stress curves of OC/EPDM nanocomposites with low ethylene contents.

to 200%, the peak is shifted towards high 2θ value [20.2°; Fig. 5(b)], and becomes sharper and stronger for 600% elongation [Fig. 5(c)]. Although the 2θ value of 20.2° is lower than 2θ value of crystalline peak in PE (21.5°), this peak should also correspond to the crystalline peak of PE segments, since the position of crystalline peak of PE shifts to low angles, with increasing propylene content in EPDM. The degree of crystallinity is a function of the extent of stretching,[18] and so, the degree of crystallinity at 600% elongation is higher than that at 200%.

By combining the results of XRD of stretched OC/J2080 samples (Fig. 5) with the corresponding stress–strain curve (Fig. 3), we noticed that the onset strain for crystallization in OC/J2080 is lower than that of the large increase in stress (about 800%). The same result was obtained in rubbers, such as natural rubber, synthetic polyisoprene rubber, poly-*cis*-1,4-butadiene rubber, and butyl rubber.[20,21] It appears that the strain-induced crystallization does not contribute to the large increase in stress. However, as proposed in the literature,[21,22] the crystallites may act as additional physical crosslinks to enable more macromolecules to orientate, and thus, the highly oriented micro-fibrillar structure and more oriented amorphous chains at high strains as strands of network should increase the tensile strength.

For comparison, XRD curves of OC/EP33 nanocomposite at different elongations are shown in Figure 6. From Figure 6, the intensity of the characteristic peaks of clay layers at 4.6, 2.0, and 1.4 nm increases slightly with the increase in elongation, indicating that the orientation of clay layers increases during the tensile process, but not as obviously as that of OC/J2080. The reason is that the higher crosslink density in OC/EP33 hinders the orientation of clay layers. The amorphous halo of EPDM, corresponding to the overlapping of

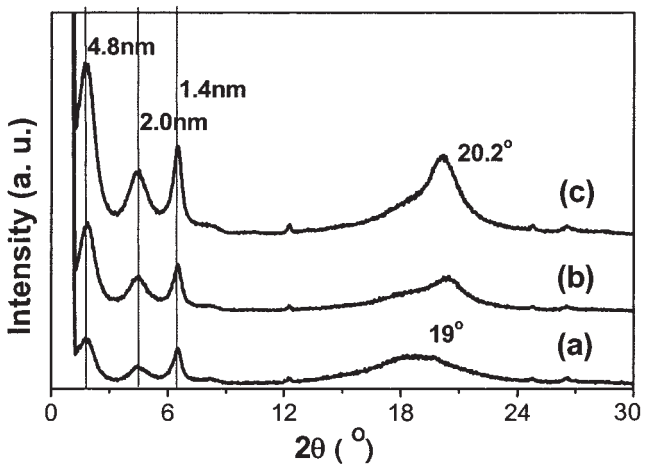

Figure 5 XRD patterns of OC/J2080 nanocomposite at different elongations: (a) before stretching; (b) at 200% elongation; and (c) at 600% elongation.

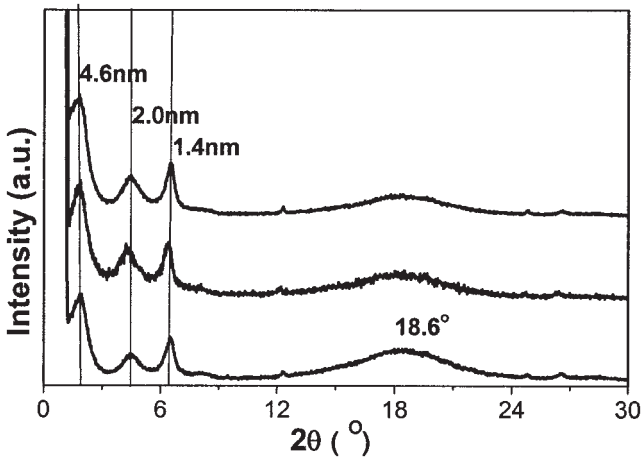

Figure 6 XRD patterns of OC/EP33 nanocomposite at different elongations: (a) before stretching; (b) at 200% elongation; (c) at 400% elongation.

amorphous PE (19.5°) and amorphous polypropylene (16.3°), did not change in both the intensity and the position, during the tensile process, suggesting that PE segments in OC/EP33 nanocomposite did not crystallize during the tensile process. The reason is that the ethylene content of 52% in EP33 is too low for PE segments to crystallize on stretching.[18] This also demonstrates indirectly the contribution of strain-induced crystallization to the large increase in stress, significantly.

CONCLUSIONS

Intercalated OC/EPDM nanocomposites have been prepared by melt blending. The ethylene content in EPDM matrix has little influence on the dispersion of OC. The addition of OC prolongs the optimum cure time and reduces the crosslink density of OC/EPDM. The decrease in crosslink density of OC/EPDM mainly contributes to higher elongation-at-break and larger permanent set than those of the corresponding pure EPDM. Strain-induced crystallization of PE segments only occurred in OC/EPDM nanocomposite with high ethylene contents (67–70%). Moreover, during the tensile process, the silicate layers arrayed more orderly, and the orientation was improved markedly. Therefore, the highly oriented micro-fibrillar structure and more oriented amorphous chains, which were caused by strain-induced crystallization of PE segments and the orientation of clay layers in OC/EPDM nanocomposites with high ethylene contents, should be responsible for larger improvement in tensile strength than that of those nanocomposites with low ethylene contents (52–52.5%)

References

1. Usuki, A.; Kojima, Y.; Kawasumi, M.; Okada, A.; Fukushima, Y.; Kurauchi, T.; Kamigaito, O. J Mater Res 1993, 8, 1179.

2. Kim, J.; Lee, D.; Oh, T.; Lee, D. J Appl Polym Sci 2003, 89, 2633.
3. Yen, T. V.; James, E. M.; Ly, H. P.; Martin, E. J Appl Polym Sci 2001, 82, 1391.
4. Alexander, B. M.; Richard, H. H. J.; Takashi, K.; Leonard, J. C.; Jeffrey, W. G. Fire Mater 2002, 26, 247.
5. Changwoon, N.; Hyune, J. R.; Wan, D. K.; Choi, S. Polym Adv Technol 2002, 13, 649.
6. Fan, J.; Liu, S.; Chen, G.; Qi, Z. J Appl Polym Sci 2002, 83, 66.
7. Xia, H.; Zhang, C.; Wang, Q. J Appl Polym Sci 2001, 80, 1130.
8. Hwu, J. M.; Jiang, J. G.; Gao, Z. M.; Xie, W.; Pan, W. P. J Appl Polym Sci 2002, 83, 1702.
9. Wu, Z.; Zhou, C.; Qi, R.; Zhang, H. J Appl Polym Sci 2002, 83, 2403.
10. Varghese, S.; Karger-Kocsis, J. J Appl Polym Sci 2004, 91, 813.
11. Wu, Y. P.; Jia, Q. X.; Yu, D. S.; Zhang, L. Q. J Appl Polym Sci 2003, 89, 3855.
12. Chang, Y.; Yang, Y.; Seunghoon, R.; Changwoon, N. Polym Int 2002, 51, 319.
13. Usuki, A.; Tukigas, A.; Kato, M. Polymer 2002, 43, 2185.
14. Zheng, H.; Zhang, Y.; Peng, Z.; Zhang, W. Polym Test 2004, 23, 217.
15. Wu, Y. P.; Ma, Y.; Wang, Y. Q.; Zhang, L. Q. Macromol Mater Eng 2004, 289, 890.
16. Gatos, K. G.; Karger-Kocsis, J. Polymer 2005, 46, 3069.
17. Dennis, H. R.; Hunter, D. L.; Chang, D.; Kim, S.; White, J. L.; Cho, J. W.; Paul, D. R. Polymer 2001, 42, 9513.
18. Bassi, I. W.; Corradihi, P.; Fagherazzi, G.; Valvassori, A. Eur Polym J 1970, 6, 709.
19. Ganter, M.; Gronski, W.; Reichert, P.; Mülhaupt, R. Rubber Chem Technol 2001, 74, 221.
20. Toki, S.; Sics, I.; Ran, S.; Liu, L.; Hsiao, B. S.; Murakami, S.; Tosaka, M.; Kohjiya, S.; Poompradub, S.; Ikeda, Y.; Tsou, A. H. Rubber Chem Technol 2004, 77, 317.
21. Trabelsi, S.; Albouy, P. A.; Rault, J. Macromolecules 2003, 36, 9093.
22. Goritz, D. Angew Makromol Chem 1992, 202–203, 309.